prosthesis

MDPI

Article

The Effect of Adding Bioactive Glass Infused with Strontium on the Surface Hardness and Surface Roughness Properties of a Heat-Cured Acrylic-Based Soft Liner

Nada Hussien Ielewi * and Faiza M. Abdul-Ameer

Department of Prosthodontics Dentistry, College of Dentistry, University of Baghdad, Baghdad 10011, Iraq; dr.fmha@codental.uobaghdad.edu.iq

* Correspondence: nada.ielewi2201@codental.uobaghdad.edu.iq

Abstract

Background: Soft liners offer a cushioning effect that aids in the healing of inflamed mucosa and allocates the relevant load in the support area of prostheses, enhancing their fit and stability. This study looks at how strontium-infused phosphate bioactive glass affects a heat-cured acrylic-based soft liner, focusing on the surface hardness and the surface roughness of the material. **Methods:** One hundred soft liner specimens were produced, with fifty specimens being designated for surface hardness testing and fifty specimens for surface roughness testing. PBG*Sr was incorporated into the soft liner at the concentrations of 1 wt.%, 3 wt.%, 5 wt.%, and 7 wt.%. Surface hardness and surface roughness were evaluated with a digital durometer for Shore A hardness and a profilometer, respectively. Fourier transform infrared spectroscopy analysis and field emission scanning electron microscopy were employed. **Results:** The Shapiro–Wilk test demonstrated that the data adhered to a normal distribution, as the *p*-values were not statistically significant. Subsequently, for statistical analyses following the one-way ANOVA, Dunnett's T3 post hoc test was employed for surface hardness, while Tukey's post hoc test was used for surface roughness. The lowest hardness value was documented in the 7 wt.% subgroup (29.040 ± 0.070), followed by the 5 wt.% subgroup (30.97 ± 0.231), and the control (40.880 ± 0.473) had the highest hardness mean value. The 7 wt.% subgroup displayed the lowest value of Ra recorded, 0.489 ± 0.077 µm, while the control subgroup showed the highest, 1.994 ± 0.168 µm. FTIR analysis suggested that the domination of physical interactions according to the analyses with the FESEM led to improved surface morphology for the 7 wt.% PBG*Sr specimens. **Conclusions:** The 7 wt.% PBG*Sr specimens exhibited the lowest surface hardness, suitable for soft lining material, and improved the surface morphology of acrylic soft liners compared with the control and other concentrations.

Keywords: soft liner; prosthetic dentistry; hardness

check for updates

Academic Editor: Marco Cicciu

Received: 11 May 2025
Revised: 13 June 2025
Accepted: 16 June 2025
Published: 22 June 2025

Citation: Ielewi, N.H.; Abdul-Ameer, F.M. The Effect of Adding Bioactive Glass Infused with Strontium on the Surface Hardness and Surface Roughness Properties of a Heat-Cured Acrylic-Based Soft Liner. *Prosthesis* **2025**, *7*, 69. https://doi.org/10.3390/prosthesis7040069

Copyright: © 2025 by the authors. Licensee MDPI, Basel, Switzerland. This article is an open access article distributed under the terms and conditions of the Creative Commons Attribution (CC BY) license (https://creativecommons.org/licenses/by/4.0/).

1. Introduction

Relining enhances the adaptation of the denture to the mucosal surface; it modifies the relationship between the underside of a denture and the denture-basal tissue, rather than serving as a temporary fix. A professional will typically conduct this process after a patient has used the denture for a specific duration. Prior to the approval of soft denture relining materials, the sole option for long-term denture relining was conventional hard denture relining materials [1]. Soft liners are often beneficial for individuals experiencing

fragile mucosa, dry mouth, bruxism, and bony undercuts when relining detachable dentures. Soft denture lining materials could be employed to address these issues, as well as others, including alveolar bone breakdown and pronounced ridges, leading to an irregular distribution of loads and resulting in tissue damage [2,3]. The elastic properties of the soft liners provide a cushioning effect by absorbing energy, which helps heal inflamed mucosa, allocate the relevant load within the field of prosthetic support, and enhance their fit and stability [4]. These materials may be classified as either interim or permanent, and they can be polymerized through auto-cure or heat-cure methods. There are five types of soft liners categorized by their chemical composition, one of which is represented by plasticized acrylic resins, which are heat-polymerized [5].

Despite the considerable progress made in the properties of soft lining materials, some limitations still persist. Soft liners are linked to various issues, such as a reduction in softness, colonization by micro-organisms, water absorption, and failure to bond with the denture base. Therefore, providers must conduct consistent clinical evaluations and the prompt replacement of soft denture liners when necessary [6].

Researchers have undertaken numerous projects to improve the characteristics of soft denture liners by introducing diverse fillers. Even in minimal quantities, the use of inorganic material nanoparticles could enhance the physical and mechanical qualities of soft denture liners [7]. Multiple compounds, which include nystatin, metallic oxide particles, azole drugs, and natural products, as well as nanoparticles such as silver, titanium dioxide (TiO_2), zinc oxide, and silica, were chosen to enhance the properties of soft lining materials [8,9]. For example, an effort was made to develop antifungal capabilities in the polyethylmethacrylate (PEMA) soft lining material by incorporating 1.0 to 2.0 percentage by weight nanoparticles of TiO_2, which effectively decreases the *C. albicans* creation of colonies in the oral cavity when compared with non-alerted PEMA material [10]. However, the introduction of substances can negatively impact the mechanical properties of the material, as their incorporation into the structure of polymer chains may influence the liner hardness [8]. After pure TiO_2 and silver-doped titanium dioxide nanoparticles were incorporated into a soft acrylic liner, researchers evaluated their antifungal activity, finding that while TiO_2 nanoparticles had no impact on the viscoelastic nature of the soft liner, silver-doped titanium dioxide nanoparticles exhibited a diminished cushioning outcome that lies within clinically reasonable limits [11]. In another study aimed at modifying silicone soft liners that used nanoparticles of silver, the specimens exhibited changes in color, which is a significant functional characteristic for dental materials, attributed to the plasmon effect of the silver nanoparticles [12].

Professor Hench developed bioactive glasses (BGs) in 1969, and they were introduced into the market as 45S5 Bioglass. BGs are attracting significant interest due to their superior properties, including bioactivity, angiogenesis, biodegradability, osteogenesis, anti-inflammatory characteristics, and antibacterial attributes [13,14]. BGs are often applied in an appropriate form as solids (bulk and porous scaffolds), powders (for coatings on biomedical devices), or composites (serving as fillers) [15]. Several dental fields, including orthodontics, periodontics, endodontics, aesthetic and restorative dentistry, and maxillofacial surgery, have utilized BGs. Additionally, several oral care items contain bioactive glasses in their formulations [16]. A notable feature of bioactive glass is its capacity to integrate therapeutic ions like copper, strontium (Sr), zinc, and fluorine into its composition. The presence of these ions can enhance the biological activities associated with bioactive glass. The presence of Sr^{2+} ions, even at minimal concentrations, enhances osteoblast differentiation while simultaneously diminishing osteoclast activity, thereby facilitating the process of creating fresh bone. Additionally, Sr^{2+} exhibits an inhibitory impact on various organisms, including *Porphyromonas gingivalis* and *Escherichia coli* [17].

The integration of bioactive glass nanoparticles within acrylic soft liners can affect critical properties, including hardness and surface roughness; according to that, this study aimed at examining the surface hardness and surface roughness properties of a heat-polymerized acrylic soft liner after the material was incorporated with phosphate bioactive glass altered by strontium (PBG*Sr). The null hypothesis suggested that neither the surface hardness nor the surface roughness would be influenced by the addition of PBG*Sr nanoparticles.

2. Materials and Methods

2.1. Phosphate Bioactive Glass Preparation

The melt–quench method was used to produce the PBG*Sr powder. The initial compounds were phosphorus pentoxide powder in 50 mol%, sodium oxide powder in 20 mol%, strontium oxide powder in 15 mol%, and calcium oxide powder in 15 mol% [18]. Raw materials were weighed and dispersed manually in a mortar to achieve a consistent combination [19]. Then, the blend was moved to an alumina crucible and heated slowly in a laboratory furnace until it was melted at 1100 °C for sixty minutes. The glass was rapidly cooled in air at 25 °C, near room temperature. The glass cooled overnight from its molten state; a powder grinder was used, and the resulting coarse processed powder was sieved under dry conditions in a planetary ball mill [20].

2.2. Mold and Specimen Preparation

Plastic disk-like models (35 mm diameter × 6 mm thickness) were used to measure both the surface hardness and the surface roughness of the specimens. Separating medium (Shanghai New Century Dental Materials Co., Ltd., Shanghai, China) was spread on the plastic models and allowed to dry up. Professional die stone extra hard type IV (Snow Rock, Seoul, Republic of Korea) was prepared following the product's guidelines (100 g powder/20 mL water), and the models were placed in the lower section of a dental flask. Half the model's thickness was inserted, while the remaining half remained above the stone surface. Once the stone material of the lower section was set up, a separating medium was applied for coating and was set aside to dry the flask, which was filled with the stone material. Once the stone proved to be completely set, the flask was opened, allowing for the removal of the plastic models and leaving spaces that served as molds to place the heat-cured acrylic soft lining material (Moonstar, Ankara, Turkey). BG nanoparticles were mixed with the liner monomer in the previously mentioned percentages through a sonication apparatus to facilitate the dispersion of the nanoparticles. The resulting BG/monomer liquid was mixed with the liner powder according to the developer's instructions (preserving the same powder/liquid ratio as recommended).

Upon achieving the requisite consistency, the mixture was manually placed into the circular mold cavities produced in the flasks and covered with polyethylene sheets, and the flasks were carefully sealed. A hydraulic press further compressed the flasks. The surplus material was eliminated before the flasks underwent curing for half an hour at 100 °C in a water bath, in accordance with the developer's guidelines. The preparation of the soft liner specimens was carried out at 25 °C, performed by one author to prevent possible errors, finished soft liner specimens in (Figure 1).

2.3. Surface Hardness Test

A digital durometer (Shore hardness tester TH200, Beijing Time High Technology Ltd., Beijing, China) coupled with its operating stand (TH200FJ) was applied for inspecting the surface hardness of the specimens. This was conducted according to the ISO 10139-2 (2016) specification [21], with a precision of $\leq \pm 1$ HA with a load of 1 kg and a cone-shaped

indenter. All the specimens (35 mm diameter × 6 mm thickness) [21] were maintained in distilled water at a temperature of 37 ± 1 °C [22] for 48 ± 1 h. The test was completed for every specimen within 2 min of its removal from water. Surface hardness values were measured digitally by determining the depth of penetration made into the material. The penetration time was 5 ± 1 s recorded at room temperature; the durometer measured five readings for every specimen, according to measurement points previously delineated: a single point in the center and four points distant from it, distributed evenly on the surface of all the given specimens. The average value of these five readings was addressed as the Shore A hardness, where readings were expressed in a range from 0 to 100 [21,22].

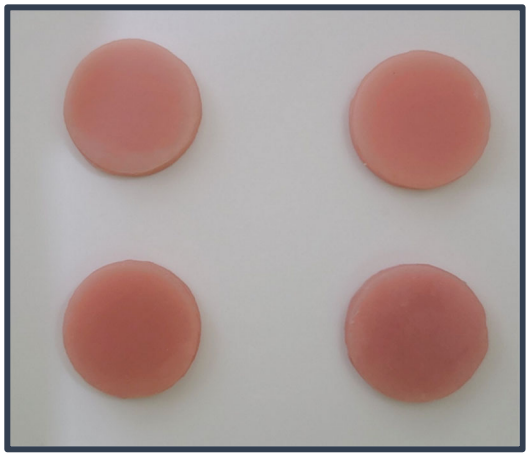

Figure 1. Soft liner specimens.

2.4. Surface Roughness Test

A profilometer (Surface roughness tester HSR210, Jinan Hensgrand Instrument Co., Ltd., Shandong, China) was utilized to calculate the surface roughness of the specimens. The device was designed with a surface analyzer (stylus). A steady force of 4 mN (0.4 g) and a tip radius of 5 µm made from diamond were used to analyze the surface profile by documenting the peaks and cavities that characterize the surface irregularities. Disk-shaped samples measuring 35 mm in diameter and 6 mm in thickness as per the ISO 10139-2 2016 standard [21,23] were stored in distilled water at a temperature of 37 ± 1 °C, and the surface roughness values (Ra) were recorded 48 ± 1 h later. For each specimen, the roughness was determined by taking the mean of the three values obtained by performing the testing on each specimen [24]. For this study, calculating the roughness was based on the arithmetic mean roughness of the profile, Ra.

2.5. Additional Tests

2.5.1. Field Emission Scanning Electron Microscope (FESEM)

For the tracing of the surface topography and the microstructure of the soft liner/PBG*Sr specimens, a field emission scanning electron microscope (InspectTM F50, FEI Company, Hillsboro, OR, USA) was utilized. An analysis was performed on random specimens, both with and without the incorporation of bioactive glass, following immersion in distilled water for a duration of 48 h. The specimens underwent a drying process and were subsequently gold-coated for 120 s on one surface by utilizing a laboratory micro plasma/metal sputtering coater (Zhengzhou CY Scientific Instrument Co., Ltd., Zhengzhou, China), with the coating duration set to 10 s. Images of the specimens were obtained at a voltage of 30 kV.

2.5.2. Fourier Transform Infrared Spectroscopy Analysis (FTIR)

The chemical structure of the PBG*Sr dry powder and soft liner specimens (the control and those modified by the percentages) after they were immersed in distal water for 48 h was analyzed using FTIR (FTIR alpha II, Bruker, Berlin, Germany) in the wavelength range of 400–4000 cm^{-1} collected at a 4 cm^{-1} resolution.

2.5.3. Statistics

According to the Shapiro–Wilk test, the data followed a normal distribution, as the test's *p*-values were not statistically significant. For the purpose of conducting statistical analyses after the one-way ANOVA (Table 1), Dunnett's T3 post hoc test for surface hardness and Tukey's post hoc test for surface roughness were utilized to assess the impact of different concentration levels on the tested properties. Statistical significance was determined by *p*-values < 0.05.

Table 1. One-way ANOVA for surface hardness and surface roughness.

Properties	Groups	Sum of Squares	df	Mean Square	F	*p*-Value
Surface hardness	Between groups	911.915	4	227.979	2428.177	0.000
	Within groups	4.225	45	0.094		
	Total	916.140	49			
Surface roughness	Between groups	0.046	5	0.009	121.552	0.000
	Within groups	0.004	54	0.000075		
	Total	0.050	59			

3. Results

3.1. Surface Hardness and Surface Roughness

According to the hardness data presented in Figure 2A, there was a noticeable decrease in all the subgroups in comparison with the control; the lowest hardness value was documented in the 7 wt.% subgroup (29.040 ± 0.070), followed by the 5 wt.% subgroup (30.97 ± 0.231), and the control (40.880 ± 0.473) had the highest hardness mean value. When comparing the PBG*Sr subgroups, there was a significant differenc ($p < 0.05$) between the control and each of the PBG*Sr subgroups.

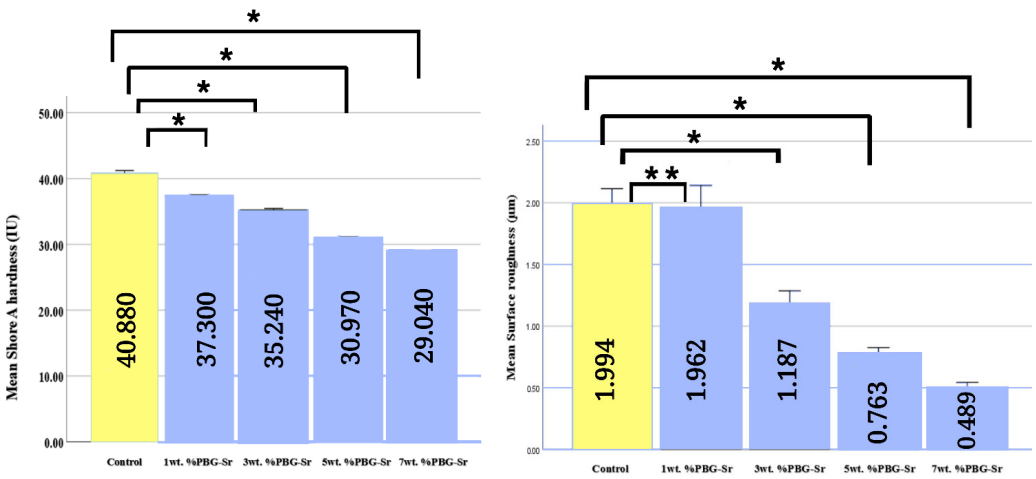

(**A**) (**B**)

Figure 2. (**A**) Shore A hardness (IU) of the control and subgroups of PBG*Sr at 1%, 3%, 5%, and 7wt.%; (**B**) surface roughness (µm) of the control and subgroups of PBG*Sr at 1%, 3%, 5%, 7wt.% * refers to a significant difference, and ** refers to a non-significant difference between the two selected groups.

The surface roughness (Ra) test results are described in Figure 2B. The 7 wt.% subgroup displayed the lowest value of Ra recorded, 0.489 ± 0.077 µm, while the control subgroup showed the highest, 1.994 ± 0.168 µm. There were significant differences in the comparisons between PBG*Sr subgroups ($p < 0.05$), except the 1 wt.% subgroup, which was non-significant compared with the control ($p > 0.05$).

3.2. Fourier Transform Infrared Spectroscopy Analysis

The FTIR spectra of PBG*Sr are provided in Figure 3A. The main bands of the spectra corresponding to 546 cm^{-1} were proposed to be the symmetrical bending and vibration of P–O–P bonds [25] [for the band at 1096 cm^{-1}, asymmetrical stretching (vas) of $(PO_3)^{2-}$ chain end; for the band at 1271 cm^{-1}, asymmetrical stretching of non-bridging oxygen atoms of O–P–O bonds, middle-of-chain $(PO2)^{-}$, and terminal oxygen bonds (P=O) in the metaphosphate Q_2 P units]. The band at 779.15 cm^{-1} correlated to the symmetric stretching vibration of P–O–P [26]. The band at 891 cm^{-1} represents the stretching of P–O–P [27]. The absorbed band at 983 cm^{-1} is connected to the symmetric stretching vibration of $(PO_2)^{-3}$ [28]. The band at 1629 cm^{-1} refers to C=O stretching [29]. The band located at 1020 cm^{-1} refers to the stretching vibration of P–O [30]. Moreover, the peak at 2924 cm^{-1} indicates the presence of the specific functional grouping CH. The bands at 2924 cm^{-1} and 2856 cm^{-1} refer to the asymmetric and symmetric stretching vibrations of CH_2, respectively [31,32]. The peak at 3432.9 refers to the stretching vibrations of O–H [33]. The absence of water as a component in the network indicates that the detected water is likely due to the phosphate glass sample's absorption of atmospheric moisture, resulting in the formation of the H–O–H band characteristic of water molecules [34].

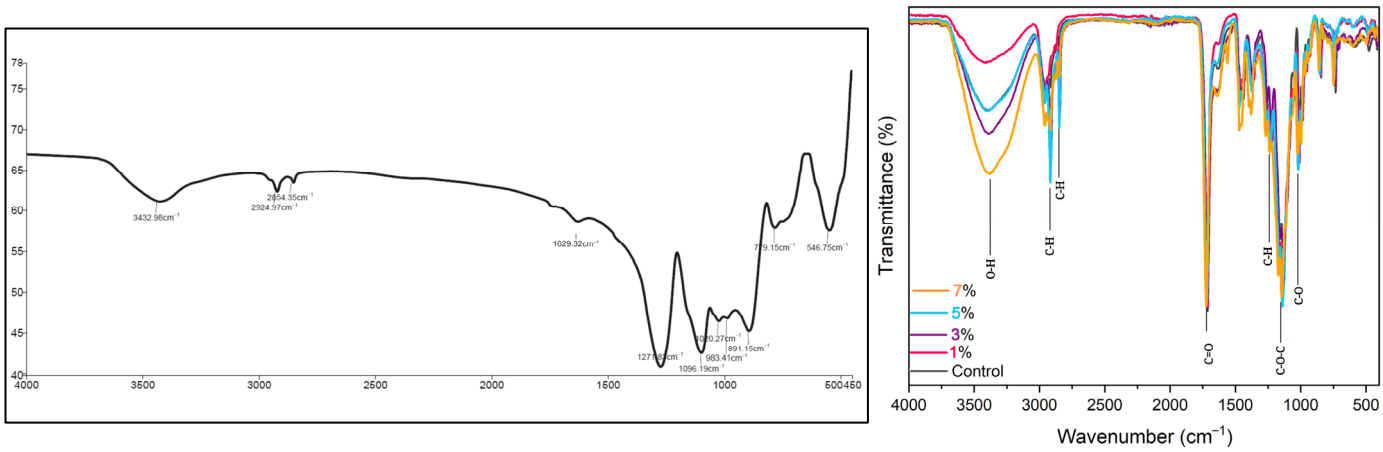

(**A**) (**B**)

Figure 3. (**A**) FTIR of PBG*Sr powder; (**B**) FTIR of soft−liner specimens at different percentages.

Soft liner/PBG*Sr specimens with different percentages (Figure 3B) showed bands at 1024 cm^{-1}, assigned to the C–O ester stretching vibrations in methoxyl [35]; at 1723 cm^{-1}, confirming the presence of carbonyl groups (C=O) [36]; at 1145 cm^{-1}, referring to the stretching vibration of the ester group (C–O–C) [37]; and at 1237 cm^{-1}, corresponding to the vibration of CH of the methyl group [38]. The absorption bands observed in the range of 3380 to 3419 cm^{-1} indicate the presence of (O–H) bonding. The additional narrow absorption at 2916 and 2918 cm^{-1}, along with the range of 2848–2850 cm^{-1}, closely corresponds to the C–H stretching of the methylene groups (CH_2) [39].

PBG*Sr seems to be incorporated in the heat-cured soft liner material without establishing chemical bonds with the matrix; no new covalent bonds are formed, suggesting that physical interactions dominate.

3.3. Field Emission Scanning Electron Microscope

The FESEM images of the surface of the specimens are presented in Figure 4. The control specimen had a rough surface with the presence of porosity and irregular depressions; the 1 wt.% specimen generally had a more homogenous surface and shallow depressions compared with the control. The 3 wt.% and 5 wt.% specimens had some agglomerations; finally, the 7 wt.% specimen indicated a smooth background with fine nanoparticle dispersion on the surface with no significant agglomeration detected.

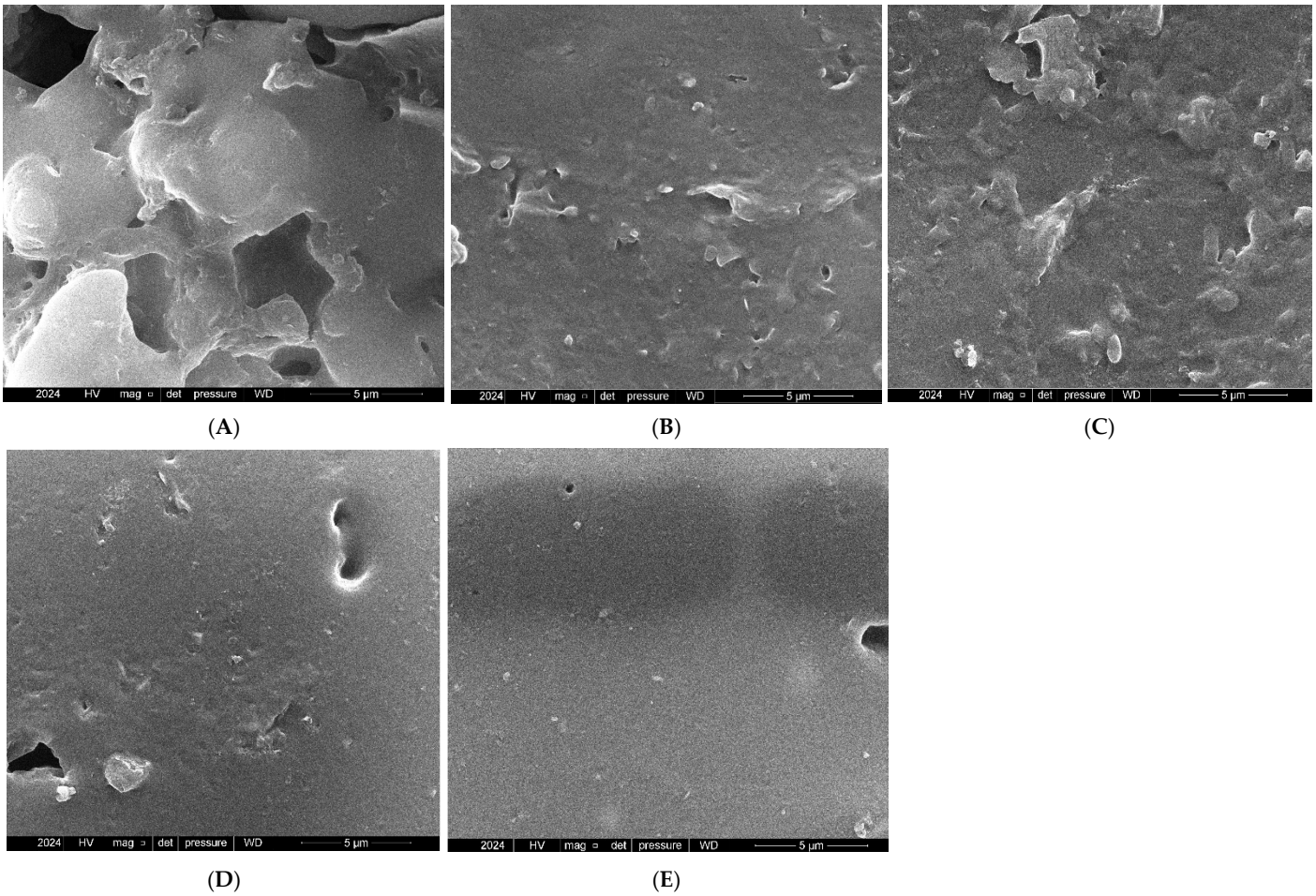

Figure 4. FESEM images of control and PBG*Sr/soft liner specimens after their immersion in distal water taken at 15,000× magnification: (**A**) control, 0 wt.%; (**B**) PBG*Sr at 1 wt.%; (**C**) PBG*Sr at 3 wt.%; (**D**) PBG*Sr at 5 wt.%; (**E**) PBG*Sr at 7 wt.%.

4. Discussion

The null hypothesis was dismissed due to the effects exerted by PBG*Sr on the two variables examined in this study. A soft lining material that hardens with time loses its therapeutic efficacy. Consequently, for the soft liner to operate well, it must retain its resilience in the oral cavity during its extended usage [40]. Hardness is directly related to the viscoelastic qualities that distribute and absorb the pressures created during clinical activity; a greater hardness value corresponds to a diminished capacity of the soft lining to absorb the force of mastication [41]. Consequently, it is preferable for such material to demonstrate a low hardness value [42]. Incorporating a non-polymer network of bonding ions diminishes the mechanical qualities of the material [43]. Including fillers in the polymer matrix enhances the material qualities of the two components if they are bonded, such as by means of salinization. Salinization is a highly effective and utilized technique for the

covalent modification of bioactive glass surfaces, with a primary aim of creating chemical bonds at the interface between inorganic components and organic biomolecules, enhancing the hydrophobicity of glass, and promoting its distribution across various liquids [44,45].

For this study, the FTIR of the specimens showed no chemical bonds, which coincides with the results of Amal et al.'s study, in which the incorporation of titanium dioxide nanoparticles into the acrylic-based soft liner culminated in a notable diminution in the surface hardness of the experimental specimens relative to their control counterparts, with no chemical interaction detected [46]. A previous study also noted a reduction in other properties of acrylic resin material with BG incorporation, which, according to the author, was due to the absence of a chemical bond between the filler and the PMMA polymer. The same situation was observed with composite materials through non-salinized fillers [43]. Furthermore, the variation in the hydrophilic and hydrophobic nature between the BG nanoparticles and the polymer leads to sub-optimal bonding interface regarding the two phases. The fundamental physical encapsulation and blending of the polymeric and inorganic phases cause a decrease in the bonding strength connecting them [47].

Research conducted by Zhao et al. mentioned that linkages between various phases may diminish when hydrophobic salinized bioactive glass BB is substituted with hydrophilic un-salinized bioactive glass 45S5 in hydrophobic resin composites [48]. The decrease in the surface hardness value noted in the 5 wt.% and 7 wt.% groups could be due to the slight aggregations that occur within the matrix of the soft liner. With the rise in nanoparticle percentages, there is a decline in properties. This finding aligns with previous investigations into the agglomeration of nanoparticles [49].

As the percentages of the BG fillers increase, they start to agglomerate within the matrix and act as centers of potential stress concentrations, which weaken the structural integrity of the soft lining material. Even in the presence of fillers, according to previous research, the weak connection between the matrix and the filler may account for their diminished mechanical capabilities [9,50]. Additionally, the rise in glass content within the soft liner exacerbates this issue. Since the bioactive glass nanoparticles in this size range (20–500 nm) exhibit a larger contact surface area, it is important to note that as their size decreases, the dispersion of these nanoparticles becomes more challenging [51]. Indeed micro-/nano-fillers tend to form stable gatherings due to the strong intermolecular forces of attraction that pull them close, such as secondary van der Waals bonds and others. The agglomerations result in reduced interfacial adhesion strength between the fillers and the matrix [52]. The current results are comparable to the outcomes observed by Jang et al., who demonstrated that the incorporation of PBG*Sr alters the surface hardness of PMMA acrylic resin material formulated with varying percentages of PBG*Sr, revealing a reduction in surface hardness values across all the testing groups as the content of PBG*Sr increases. In their study, 7.5 wt.% and 15 wt.% PBG*Sr exhibited the lowest surface hardness values when compared with the control group ($p < 0.05$), indicating that PBG*Sr may compromise interfacial bonding [53]. The results gathered in this paper were lower than the typical measurements recorded for acrylic soft lining according to Chladek, which is attributed to the fact that the tests were carried out on the specimens at 37 °C, in contrast to other studies, which took place at ambient temperature [54]. The outcome is also contingent upon the composition and specific type of substances with low molecular masses, including plasticizers and ethanol, incorporated into soft lining material. The higher the mass of those included in the developed material, the lesser the initial hardness of the material; however, additional compounds, such as antifungal additives, may have detrimental effects on the hardness of soft lining materials [55].

Decreasing the particle size of the BG fillers leads to a better surface finish of the consequent composite material. Yet, a smaller particle size (5 nm to 1 μm) can lead to

issues, including an increased surface area and a higher dissolution rate of bioactive glass, along with the absorption of CO_2 and H_2O from the surrounding environment [44]. The diminutive size of the nanoparticles enables them to occupy the micro-gaps present between the polymer chains, resulting in a uniform nanoparticle-containing matrix following heat polymerization [56]. Surface morphology was analyzed using FESEM; higher percentages (5 wt.% and 7 wt.%) displayed smoother surfaces with minimized inconsistencies and particles on the surface. The decrease in surface roughness observed with water submersion could be associated with the materials' chemistry and intrinsic properties. Further, the reduction in soluble components following submersion in water leads to the creation of voids and pores. The increase in these pores leads to the formation of craters, while the edges of these craters can diminish, which leads to a smoother appearance of the specimens [57]. In alignment with the findings by Raghunath et al., the incorporation of varying percentages of cerium oxide nanoparticles into a soft liner revealed that decreasing the percentages resulted in rougher surfaces with apparent particles, whereas higher percentages displayed smoother surfaces with fewer particles when improvements in surface morphology were examined through FESEM, indicating that the percentage affects surface characteristics and uniformity [58].

The roughness of a material is largely determined by its intrinsic characteristics, the ability of the operator, and the polishing techniques employed. Consequently, variations in the roughness estimates shared in other research can be attributed to differences in methodologies, such as the testing methods and the techniques used for measuring surface roughness [59]. The present results distinguish themselves from those of Gad et al.'s study, in which no differences were found in the surface roughness of heat-polymerized denture base materials with the addition of bioactive glass [60]. Although the 7 wt.% experimental specimens exhibited a more improved surface compared with the control and other percentages, according to previous studies, the substrate surface must have a standard surface roughness of less than 0.2 μm to avoid influencing the extent of biofilm development [61]. Compared with soft liners made of silicone, soft liners made of methacrylate have rougher surfaces; however, the type of polymerization influenced the substrate roughness, and accordingly, heat-polymerized liners exhibited reduced surface roughness [17].

Even though the decrease in surface roughness measurements still exceeded the clinically advised limit of 0.2 μm, this is consistent with observations by others who have faced difficulties in achieving this degree of uniformity in practical applications. Although sophisticated methods have shown that it is possible to reach Ra < 0.2 μm under laboratory conditions, their use in clinical settings is still restricted because of various limitations. During in vivo experimentation utilizing adult rat models to examine the surface roughness of acrylic and silicone-based soft liners, the average surface roughness of each material evaluated surpassed the threshold deemed clinically optimal (0.2 μm) [62].

Note that the inclusion of PBG*Sr did not alter the color of the soft liner utilized in the study, considering the significance of aesthetic characteristics in dental materials. The selection of the medium can impact the outcomes, and the common media employed in studies include water and artificial saliva. Findings suggest that using distilled water delivers lower mechanical values and higher liquid absorption compared with storage in artificial saliva, although these differences do not reach statistical significance. This indicates that employing water with distillation in these studies was a logical decision, as water exhibits, at the very least, a comparable degrading effect when contrasted to artificial saliva. Nevertheless, the two liquids discussed do not entirely represent actual conditions [63].

5. Conclusions

Following the incorporation of 1 wt.%, 3 wt.%, 5 wt.%, and 7 wt.% PBG*Sr, the Shore hardness and surface roughness of these subgroups exhibited a substantial reduction compared with the control specimens, all of them within the acceptable clinical usage of the materials. PBG*Sr incorporation at 7 wt.% improves the surface morphology of acrylic soft liners, outperforming the control and other percentages. Although the reduction in surface roughness did not achieve the threshold generally advised for limiting microbial adhesion (<0.2 μm), the observed improvement would provide possible advantages in reducing plaque and hygiene preservation relative to conventional liners. The same 7 wt.% PBG*Sr subgroup exhibited the lowest value of surface hardness, maintaining the liner's essential functions, including resilience and cushioning.

Future research should focus on surface modification approaches in BG, especially silanization, to optimize the clinical performance of customized liners. A balanced approach is necessary to enhance both the therapeutic effects of bioactive glass and the mechanical properties of these liners; in order to achieve that, it would be interesting to perform partial silanization. This could contribute to improvements in mechanical properties, particle dispersion, and long-term stability. This study focused solely on a single soft lining material and a specific formulation of phosphate bioactive glass; other properties of soft liners, such as dimensional stability and biocompatibility, require consideration. The investigation was limited to the baseline measurements of surface hardness and roughness; potential variations over time and with water deserve further attention.

Additional exploration of alternative bioactive glass compositions and the examination of different forms, including silicate-based and borate-based varieties, are necessary to enhance our understanding of their interactions and optimize the material properties of soft liners. It is crucial to evaluate the biological reaction of oral tissues to bioactive glasses, especially with regard to bone remodeling, abutment teeth, residual ridges, and mucosal health. It is necessary to thoroughly examine how bioactive liners interact with the surrounding hard tissues, especially with regard to their capacity for remineralization and any unforeseeable detrimental effects.

Author Contributions: Conceptualization, N.H.I. and F.M.A.-A.; methodology, N.H.I.; software, N.H.I.; validation, F.M.A.-A.; formal analysis, N.H.I.; investigation, N.H.I.; resources, N.H.I.; data curation, N.H.I.; writing—original draft preparation, N.H.I.; writing—review and editing, F.M.A.-A.; visualization, F.M.A.-A.; supervision, F.M.A.-A.; project administration, N.H.I.; funding acquisition, N.H.I. All authors have read and agreed to the published version of the manuscript.

Funding: This research received no external funding.

Institutional Review Board Statement: Not applicable.

Informed Consent Statement: Not applicable.

Data Availability Statement: Data is available upon reasonable request to authors.

Acknowledgments: The authors wanted to give thanks and gratitude to the College of Dentistry, University of Baghdad, for providing technical support.

Conflicts of Interest: The authors declare no conflicts of interest.

References

1. Hasegawa, Y.; Minakuchi, H.; Nishimura, M.; Nishio, K.; Yoshioka, F.; Ishii, T.; Watanabe, T.; Nishiyama, Y.; Sato, Y.; Yoshida, K.; et al. Effect of soft denture liners on complete denture treatments: A systematic review. *J. Prosthodont. Res.* **2024**, *68*, 493–510. [CrossRef] [PubMed]
2. Dutta, A.; Kumar, S.; Chowdhary, Z.; Bumb, P.; Kumar, C. Effect of Water Sorption and Solubility on Two Soft Denture Lining Materials Stored in Three Different Mediums. *Int. J. Prosthodont. Restore Dent.* **2023**, *13*, 129–136.

3. Memon, M.R.; Memon, H.; Shoro, M.; Bhurgri, H.; Issrani, R.; Iqbal, A.; Khattak, O.; Altassan, M.; Almabadi, A.A.; Sultan, S.E.S.; et al. Effectiveness of Chitosan versus Natural Aloe Vera on Candida Adherence in Denture Soft Lining Material. *Scientifica* **2024**, *2024*, 9918914. [CrossRef] [PubMed]
4. Alqutaibi, A.Y.; Alnazzawi, A.A.; Farghal, A.E.; Bakr, R.M.; Mahmoud, I.I. Impact of acrylic and Silicone-Based Soft-Liner materials on biting force and quality of life of the complete denture wearers: A randomized clinical trial. *J. Clin. Med.* **2023**, *12*, 2073. [CrossRef]
5. Hamedirad, F.; Alikhasi, M.; Hasanzade, M. The effect of sandblasting on bond strength of soft liners to denture base resins: A Systematic Review and Meta-Analysis of In Vitro Studies. *Int. J. Dent.* **2021**, *2021*, 5674155. [CrossRef]
6. Hashem, M.I. Advances in soft denture liners: An update. *J. Contemp. Dent. Pract.* **2015**, *16*, 314–318.
7. Jasim, B.S.; Alalwan, H.K.A.; Fatalla, A.A.; Al-Samaray, M.E. The impact of modified metallic nanoparticles on thermomechanical properties of PMMA soft liner. *Nano Biomed. Eng.* **2023**, *15*, 408–415. [CrossRef]
8. Songsang, N.; Anunmana, C.; Pudla, M.; Eiampongpaiboon, T. Effects of Litsea cubeba Essential Oil Incorporated into Denture Soft Lining Materials. *Polymers* **2022**, *14*, 3261. [CrossRef]
9. Habibzadeh, S.; Omidvaran, A.; Eskandarion, S.; Shamshiri, A.R. Effect of Incorporation of Silver Nanoparticles on the Tensile Bond Strength of a Long term Soft Denture Liner. *Eur. J. Dent.* **2020**, *14*, 268–273. [CrossRef]
10. Ahmed, A.Q.; Al-Hmedat, S.J.A.Z.; Hanweet, D.M.; Haider, J. Assessing the Antifungal Activity of a Soft Denture Liner Loaded with Titanium Oxide Nanoparticles (TiO_2 NPs). *Dent. J.* **2023**, *11*, 90. [CrossRef]
11. Waly, G.H. Effect of incorporating undoped or silver-doped photocatalytic titanium dioxide on the antifungal effect and dynamic viscoelastic properties of long-term acrylic denture liners. *Future Dent. J.* **2018**, *4*, 8–15. [CrossRef]
12. Chladek, G.; Mertas, A.; Barszczewska-Rybarek, I.; Nalewajek, T.; Zmudzki, J.; Król, W.; Lukaszczyk, J. Antifungal activity of denture soft lining material modified by Silver Nanoparticles—A pilot study. *Int. J. Mol. Sci.* **2011**, *12*, 4735–4744. [CrossRef] [PubMed]
13. Zeimaran, E.; Pourshahrestani, S.; Fathi, A.; Razak, N.A.B.A.; Kadri, N.A.; Sheikhi, A.; Baino, F. Advances in bioactive glass-containing injectable hydrogel biomaterials for tissue regeneration. *Acta Biomater.* **2021**, *136*, 1–36. [CrossRef] [PubMed]
14. Pantulap, U.; Arango-Ospina, M.; Boccaccini, A.R. Bioactive glasses incorporating less-common ions to improve biological and physical properties. *J. Mater. Sci. Mater. Med.* **2021**, *33*, 3. [CrossRef]
15. Cannio, M.; Bellucci, D.; Roether, J.A.; Boccaccini, D.N.; Cannillo, V. Bioactive Glass Applications: A Literature Review of human clinical trials. *Materials* **2021**, *14*, 5440. [CrossRef]
16. Jafari, N.; Habashi, M.S.; Hashemi, A.; Shirazi, R.; Tanideh, N.; Tamadon, A. Application of bioactive glasses in various dental fields. *Biomater. Res.* **2022**, *26*, 31. [CrossRef]
17. Silva, A.V.; Gomes, D.D.S.; De Sousa Victor, R.; De Lima Santana, L.N.; Neves, G.A.; Menezes, R.R. Influence of strontium on the biological behavior of bioactive glasses for bone regeneration. *Materials* **2023**, *16*, 7654. [CrossRef]
18. Go, H.B.; Lee, M.J.; Seo, J.Y.; Byun, S.Y.; Kwon, J.S. Mechanical properties and sustainable bacterial resistance effect of strontium-modified phosphate-based glass microfiller in dental composite resins. *Sci. Rep.* **2023**, *13*, 17763. [CrossRef]
19. Gobbo, V.A.; Parihar, V.S.; Prato, M.; Kellomäki, M.; Vernè, E.; Spriano, S.; Massera, J. Surface modification of silicate, borosilicate and phosphate bioactive glasses to improve/control protein adsorption: PART I. *Ceram. Int.* **2022**, *49*, 1261–1275. [CrossRef]
20. Ryu, J.H.; Mangal, U.; Lee, M.J.; Seo, J.Y.; Jeong, I.J.; Park, J.Y.; Na, J.Y.; Lee, K.J.; Yu, H.S.; Cha, J.K.; et al. Effect of strontium substitution on functional activity of phosphate-based glass. *Biomater. Sci.* **2023**, *11*, 6299–6310. [CrossRef]
21. *ISO 10139-2:2016*; Dentistry—Soft Lining Materials for Removable Dentures—Part 2: Materials for Long-Term Use. ISO: Geneva, Switzerland, 2016.
22. Ivana, I.; Nasution, I.D.; Nasution, D.Y. Effect of sealer coating on hardness and water sorption data of soft denture lining materials. *Data Brief* **2021**, *36*, 107083. [CrossRef] [PubMed]
23. Herla, M.; Boening, K.; Meissner, H.; Walczak, K. Mechanical and Surface Properties of Resilient Denture Liners Modified with Chitosan Salts. *Materials* **2019**, *12*, 3518. [CrossRef] [PubMed]
24. Kutlu, I.U.; Yanikoğlu, N.D.; Kul, E.; Duymuş, Z.Y.; Sağsöz, N.P. Effect of sealer coating and storage methods on the surface roughness of soft liners. *J. Prosthet. Dent.* **2015**, *115*, 371–376. [CrossRef]
25. Stoch, P.; Stoch, A.; Ciecinska, M.; Krakowiak, I.; Sitarz, M. Structure of phosphate and iron-phosphate glasses by DFT calculations and FTIR/Raman spectroscopy. *J. Non-Cryst. Solids* **2016**, *450*, 48–60. [CrossRef]
26. Stuart, B.W.; Stan, G.E.; Popa, A.C.; Carrington, M.J.; Zgura, I.; Necsulescu, M.; Grant, D.M. New solutions for combatting implant bacterial infection based on silver nano-dispersed and gallium incorporated phosphate bioactive glass sputtered films: A preliminary study. *Bioact. Mater.* **2021**, *8*, 325–340. [CrossRef]
27. Rajkumar, G.; Rajendran, V.; Aravindan, S. Role of MgO on the HAp forming ability in phosphate based glasses. *Ceram. Int.* **2012**, *38*, 3781–3790. [CrossRef]
28. Ghanavati, S.; Petit, L.; Massera, J. New Mg/Sr phosphate bioresorbable glass system with enhanced sintering properties. *J. Non-Cryst. Solids* **2023**, *616*, 122446. [CrossRef]

29. Cai, Z.; Liu, X.; Hu, M.; Meng, Y.; Zhao, J.; Tan, Y.; Luo, X.; Wang, C.; Ma, J.; Sun, Z.; et al. In Situ Enzymatic Reaction Generates Magnesium-Based Mineralized Microspheres with Superior Bioactivity for Enhanced Bone Regeneration. *Adv. Healthc. Mater.* **2023**, *12*, e2300727. [CrossRef]
30. Elgharbawy, H.; Hemeda, O.M.; Henaish, A.M.A. Exploring the potential of new boron-phosphate bioactive glass doped with lanthanum and zinc oxides for bone regeneration: In vitro study. *J. Mol. Struct.* **2024**, *1307*, 137958. [CrossRef]
31. Elangovan, U.; Anbarasu, K.; Shanmugam, R.; Veeramuthu, D.; John, J.G. Biological Properties of Mycosynthesized Novel Strontium Oxide Nanoparticles from Biomass Free Filtrate of Endophytic Fungus Aspergillus sp. LCJ315. *BioNanoScience* **2024**, *14*, 2145–2158. [CrossRef]
32. Sun, L.; Li, S.; Yang, K.; Wang, J.; Li, Z.; Dan, N. Polycaprolactone strengthening keratin/bioactive glass composite scaffolds with double cross-linking networks for potential application in bone repair. *J. Leather Sci. Eng.* **2022**, *4*, 1. [CrossRef]
33. Ikhmayies, S.J. *Advances in Glass Research*; Springer International Publishing: Cham, Switzerland, 2023.
34. Mohan Babu, M.; Syam Prasad, P.; Hima Bindu, S.; Prasad, A.; Venkateswara Rao, P.; Putenpurayil Govindan, N.; Veeraiah, N.; Özcan, M. Investigations on Physico-Mechanical and Spectral studies of Zn^{2+} doped P_2O_5-Based bioglass System. *J. Compos. Sci.* **2020**, *4*, 129. [CrossRef]
35. Popescu, M.C.; Froidevaux, J.; Navi, P.; Popescu, C.M. Structural modifications of Tilia cordata wood during heat treatment investigated by FT-IR and 2D IR correlation spectroscopy. *J. Mol. Struct.* **2012**, *1033*, 176–186. [CrossRef]
36. Aziz, R.; Sadoon, M. Surface hardness and fourier transform infrared spectroscopical characterization of bioactive modified chairside hard denture reliner. *Al-Rafidain Dent. J.* **2024**, *24*, 231–247. [CrossRef]
37. Noori, A.A.; Jaber, M.A. Evaluation the effect of incorporation of different herbal extract powders (*Either neem* or *Aloe vera*) on thermal conductivity and shear bond strength of acrylic soft denture liner material. *Tikrit J. Dent. Sci.* **2023**, *10*, 35–46. [CrossRef]
38. Ramírez-Hernández, A.; Aguilar-Flores, C.; Aparicio-Saguilán, A. Fingerprint analysis of FTIR spectra of polymers containing vinyl acetate. *Dyna* **2019**, *86*, 198–205. [CrossRef]
39. Habibi, H.; Alam, A.S.; Prasetyawan, O.; Supriyadi, G. FTIR and SEM analysis of breakdown XLPE cable insulation. In Proceedings of the 2021 3rd International Conference on High Voltage Engineering and Power Systems (ICHVEPS), Bandung, Indonesia, 5–6 October 2021; pp. 314–317. [CrossRef]
40. Alsaiari, M.; Khan, G.; Khan, M.A.; Liaqat, S.; Alkorbi, A.S.; Irfan, M.; Rizk, M.A.; Muhammad, N. Evaluation of the effect of lignin on mechanical, water sorption, and antifungal properties of silicone based denture soft liners. *Silicon* **2023**, *15*, 6121–6134. [CrossRef]
41. Kreve, S.; Reis, A.C.D. Denture Liners: A Systematic Review relative to adhesion and mechanical properties. *Sci. World J.* **2019**, *2019*, 6913080. [CrossRef]
42. Alsaiari, M.; Roghani, K.; Liaqat, S.; Alkorbi, A.S.; Sharif, F.; Irfan, M.; Rizk, M.A.; Uroos, M.; Ahmad, N.; Muhammad, N. Effect of ionic liquids on mechanical, physical, and antifungal properties and biocompatibility of a soft denture lining material. *ACS Omega* **2023**, *8*, 27300–27311. [CrossRef]
43. Raszewski, Z.; Chojnacka, K.; Mikulewicz, M. Preparation and characterization of acrylic resins with bioactive glasses. *Sci. Rep.* **2022**, *12*, 16624. [CrossRef]
44. Tiskaya, M.; Shahid, S.; Gillam, D.; Hill, R. The use of bioactive glass (BAG) in dental composites: A critical review. *Dent. Mater.* **2021**, *37*, 296–310. [CrossRef] [PubMed]
45. Deshmukh, K.; Kovářík, T.; Křenek, T.; Docheva, D.; Stich, T.; Pola, J. Recent advances and future perspectives of sol–gel derived porous bioactive glasses: A review. *RSC Adv.* **2020**, *10*, 33782–33835. [CrossRef] [PubMed]
46. Ahmed, A.Q.; Ali, M.M.M. The Influence of Titanium Dioxide Nanoparticles Incorporation into Soft Denture Lining Material on Candida albicans Adherence and Some Mechanical and Physical Properties. *J. Pure Appl. Microbiol.* **2018**, *12*, 783–791. [CrossRef]
47. Chen, M.; Wang, Y.; Yuan, P.; Wang, L.; Li, X.; Lei, B. Multifunctional bioactive glass nanoparticles: Surface-Interface decoration and biomedical applications. *Regen. Biomater.* **2024**, *11*, rbae110. [CrossRef]
48. Zhao, H.; Tsigkou, O.; Chen, X. The effect of bioactive glass particle size on viscosity, stickiness and packability of resin composites. *Next Mater.* **2024**, *5*, 100265. [CrossRef]
49. Altarazi, A.; Haider, J.; Alhotan, A.; Silikas, N.; Devlin, H. 3D printed denture base material: The effect of incorporating TiO_2 nanoparticles and artificial ageing on the physical and mechanical properties. *Dent. Mater.* **2023**, *39*, 1122–1136. [CrossRef]
50. Lopes, P.; Garcia, M.; Fernandes, M.; Fernandes, M. Properties and osteoblast cytocompatibility of self-curing acrylic cements modified by glass fillers. *J. Biomater. Appl.* **2012**, *28*, 498–513. [CrossRef]
51. Vichery, C.; Nedelec, J.M. Bioactive glass nanoparticles: From synthesis to materials design for biomedical applications. *Materials* **2016**, *9*, 288. [CrossRef]
52. Nayak, C.; Balani, K. Effects of reinforcements and gamma-irradiation on wear performance of ultra-high molecular weight polyethylene as acetabular cup liner in hip-joint arthroplasty: A review. *J. Appl. Polym. Sci.* **2021**, *138*, 51275. [CrossRef]
53. Jang, E.J.; Hong, Y.J.; Jeong, Y.H.; Kim, K.E.; Jo, E.S.; Lee, M.J.; Yang, S.Y. In vitro antifungal and physicochemical properties of polymerized acrylic resin containing strontium-modified phosphate-based glass. *BMC Oral Health* **2024**, *24*, 775. [CrossRef]

54. Chladek, G.; Kalamarz, I.; Pakieła, W.; Barszczewska-Rybarek, I.; Czuba, Z.; Mertas, A. A Temporary Acrylic Soft Denture Lining Material Enriched with Silver-Releasing Filler-Cytotoxicity, Mechanical and Antifungal Properties. *Materials* **2024**, *17*, 902. [CrossRef] [PubMed]
55. Barszczewska-Rybarek, I.; Kula, P.; Chladek, G. Review of the Anti-Candida albicans Activity and Physical Properties of Soft Lining Materials Modified with Polyene Antibiotics, Azole Drugs, and Chlorohexidine Salts. *Materials* **2024**, *17*, 5383. [CrossRef] [PubMed]
56. Alhotan, A.; Raszewski, Z.; Chojnacka, K.; Mikulewicz, M.; Kulbacka, J.; Alaqeely, R.; Mirdad, A.; Haider, J. Evaluating the Translucency, Surface Roughness, and Cytotoxicity of a PMMA Acrylic Denture Base Reinforced with Bioactive Glasses. *J. Funct. Biomater.* **2023**, *15*, 16. [CrossRef] [PubMed]
57. Bueno, M.G.; De Sousa, E.J.B.; Hotta, J.; Porto, V.C.; Urban, V.M.; Neppelenbroek, K.H. Surface properties of temporary soft liners modified by minimum inhibitory concentrations of antifungals. *Braz. Dent. J.* **2017**, *28*, 158–164. [CrossRef]
58. Raghunath, S.M.; Jei, J.B.; Muthukumar, B. Characterization of nanoceria-modified silicone soft liners: Surface morphology, hardness, wettability, cytotoxicity, and antifungal properties in artificial saliva—An in vitro study. *J. Oral Biol. Craniofacial Res.* **2024**, *14*, 614–619. [CrossRef]
59. Naser, H.J.; Abdul-Ameer, F.M. Evaluating the effect of lemongrass essential oil addition on some properties of heat cure acrylic Soft-Lining material. *Med. J. Babylon.* **2022**, *19*, 646–652. [CrossRef]
60. Gad, M.M.; Abu-Rashid, K.; Alkhaldi, A.; Alshehri, O.; Khan, S.Q. Evaluation of the effectiveness of bioactive glass fillers against Candida albicans adhesion to PMMA denture base materials: An in vitro study. *Saudi Dent. J.* **2022**, *34*, 730–737. [CrossRef]
61. Le, P.H.; Linklater, D.P.; Medina, A.A.; MacLaughlin, S.; Crawford, R.J.; Ivanova, E.P. Impact of multiscale surface topography characteristics on Candida albicans biofilm formation: From cell repellence to fungicidal activity. *Acta Biomater.* **2024**, *177*, 20–36. [CrossRef]
62. Bail, M.; Jorge, J.H.; Urban, V.M.; Campanha, N.H. Surface roughness of acrylic and Silicone-Based soft liners: In vivo study in a Rat model. *J. Prosthodont.* **2013**, *23*, 146–151. [CrossRef]
63. Chladek, G.; Pakieła, K.; Pakieła, W.; Żmudzki, J.; Adamiak, M.; Krawczyk, C. Effect of antibacterial Silver-Releasing filler on the physicochemical properties of Poly(Methyl methacrylate) denture base material. *Materials* **2019**, *12*, 4146. [CrossRef]

Disclaimer/Publisher's Note: The statements, opinions and data contained in all publications are solely those of the individual author(s) and contributor(s) and not of MDPI and/or the editor(s). MDPI and/or the editor(s) disclaim responsibility for any injury to people or property resulting from any ideas, methods, instructions or products referred to in the content.